Polarization-based isotope-selective two-color photoionization of atomic samarium using broadband lasers

A. U. Seema · Asawari D. Rath ·
P. K. Mandal · Vas Dev

Abstract An isotope separation method based on polarization selection rules is applied to atomic samarium by using two-color resonance ionization spectroscopy with broadband lasers. In this method, odd isotopes with nonzero nuclear spin are selectively excited, while even isotopes with zero nuclear spin are prohibited from excitation using two parallel linearly polarized lasers. We have identified a two-color excitation scheme 0 cm^{-1} $(J = 0) \rightarrow 15650.5$ cm^{-1} $(J = 1) \rightarrow 33116.8$ cm^{-1} $(J = 1) \rightarrow$ Sm$^+$ for selective excitation of the odd isotopes of Sm I. Using this scheme, selective excitation of odd isotopes of Sm I ([147]Sm and [149]Sm) with an isotopic selectivity better than 40 has been demonstrated. In addition, the effect of different polarization states of the excitation lasers and relative polarization angle between them on the selectivity of odd isotopes has also been studied. The dependence of the even mass isotope signal on the relative polarization angle followed $\sin^2\theta$, which is in excellent agreement with theoretical predictions.

1 Introduction

In laser isotope separation (LIS) process, isotope-selective photoionization of the target isotope is generally achieved by utilizing the isotopic shift or the difference in the hyperfine structure of different isotopes using narrow-band lasers. This method puts stringent condition on the laser bandwidths and the atomic beam parameters especially when the isotope shifts are small and the hyperfine

A. U. Seema (✉) · A. D. Rath · P. K. Mandal · V. Dev
Laser and Plasma Technology Division, Bhabha Atomic Research
Centre, Trombay, Mumbai 400085, India
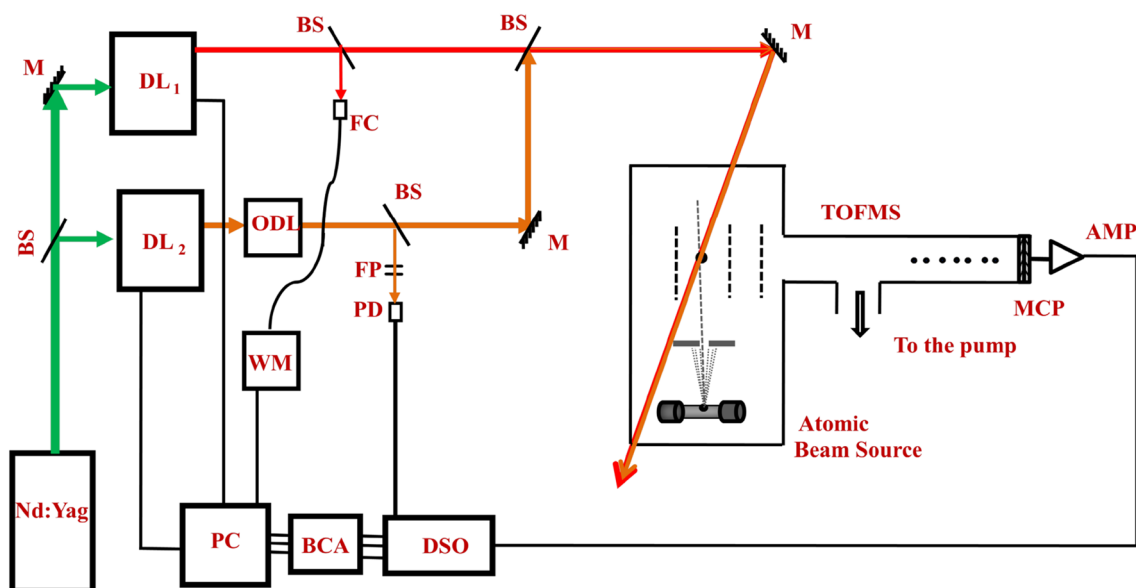e-mail: auseema@barc.gov.in

spectra are overlapping. An alternative isotope separation method based on polarization selection rules using broadband lasers has been previously applied for separation of odd and even isotopes of Zr, Gd, and Yb where the isotope shifts are small and the hyperfine spectra are complex [1–8]. Isotope separation of many of these elements is of great importance to nuclear industry [1–6]. In this method, odd isotopes with nonzero nuclear spin are selectively excited, while even isotopes with zero nuclear spin are prohibited from excitation by judiciously choosing a proper excitation sequence of angular momenta of the levels and the laser polarizations. However, this method is applicable to elements having states with low total angular momentum (J values).

Atomic samarium (Sm I) has seven naturally abundant isotopes [144]Sm (3.1 %), [147]Sm (15 %), [148]Sm (11.3 %), [149]Sm (13.8 %), [150]Sm (7.4 %), [152]Sm (26.6 %), and [154]Sm (22.6 %). Among these, [149]Sm, with high thermal neutron absorption cross section (40,140 barns), is a promising candidate as burnable poison in nuclear reactors [9]. The use of natural samarium as a burnable poison was discarded previously because of the large residual negative reactivity worth of samarium isotopes and their daughter products at the end of life of the fuel. Recently, Renier et al. [10] have investigated the potential benefits of using enriched samaria (Sm$_2$O$_3$) as a burnable poison in the fuel pellets of PWRs and shown that the use of Sm enriched in [149]Sm has greatly reduced this residual absorber problem.

In this paper, we report isotope-selective photoionization of atomic samarium (Sm I) using two-color resonance ionization polarization spectroscopy with broadband lasers. We have identified a two-color excitation scheme 0 cm^{-1} $(J = 0) \rightarrow 15650.5$ cm^{-1} $(J = 1) \rightarrow 33116.8$ cm^{-1} $(J = 1) \rightarrow$ Sm$^+$ for selective excitation of the odd isotopes of Sm I [11, 12]. Using this scheme, selective excitation of

Fig. 1 Schematic of the experimental setup

odd isotopes of Sm I (^{147}Sm and ^{149}Sm) with isotopic selectivity better than 40 has been demonstrated using broadband lasers. In addition, we have also studied the effect of different polarization states of the excitation lasers and relative polarization angle between them on the selectivity. The method has the unique advantage that it does not demand a high spectroscopic resolution and thus has the benefit of using broadband lasers and thermally distributed atomic beams. These inherent characteristics make the method highly useful for the separation of odd isotopes with small isotope shifts and broad hyperfine structures.

2 Experimental

The schematic of the experimental setup is shown in Fig. 1. It consists of two pulsed dye lasers (Quantel, TDL-90) pumped by an Nd:YAG laser, a wavelength meter (High Finesse WS6), Fabry-Perot etalon (FP), a photodiode (PD), a high temperature atomic vapor source coupled to a time-of-flight mass spectrometer (TOF-MS), a digital storage oscilloscope (DSO), and boxcar averagers (BCA) for signal processing and a computer (PC) for signal recording. A frequency-doubled Nd:YAG laser at 532 nm is used to pump two dye lasers DL_1 and DL_2 to provide tunable output at wavelengths λ_1 and λ_2, respectively. Both lasers have a pulse duration ~6 ns, typical line widths of ~0.20 cm^{-1}, and pulse energies of ~2 mJ/pulse. The DL_2 is temporally delayed with respect to DL_1 by 8 ns (i.e., more than the dye laser pulse width) using an optical delay line in order to ensure sequential absorption of photons.

DCM and Rh6G dyes are used in DL_1 and DL_2 lasers to produce laser photons at desired wavelengths λ_1 and λ_2, respectively. Spatially overlapped DL_1 and DL_2 lasers are then sent through a samarium atomic beam formed in the high-vacuum atomic beam generator that is coupled to the TOFMS. The typical laser fluence in the interaction zone is ~100 μJ cm^{-2} for DL_1 and that of DL_2 is variable from 200 μJ cm^{-2} to 1 mJ cm^{-2}. The atomic vapor of Sm is produced by resistively heating few hundred milligrams of Sm metal to ~800°K in a high-vacuum chamber maintained at a pressure of ~10^{-6} mbar. The Sm vapor effusing out of the oven orifice of 1 mm diameter is further apertured by using a fixed aperture of diameter 3 mm at a distance of 15 mm from the oven orifice. The typical number density of Sm in the laser–atom interaction zone is ~10^9 atoms cm^{-3}. The reduced Doppler width of the atomic absorption line in the interaction zone is ~100 MHz. The photoions generated in the interaction region are extracted by a DC electric field of strength 150 V cm^{-1} and then introduced into the flight tube of the TOFMS. After travelling a field-free-flight region of 90 cm, the photoions are detected by a microchannel plate (MCP) detector. The detector output signal is amplified using a preamplifier (gain ~100 and a bandwidth ~100 MHz) before it is fed to a boxcar averager for processing. The output of the boxcar averager is then transferred to a computer for storage and further data analysis. A fraction (~4 %) of the DL_2 is made to pass through a FP etalon (free spectral range = 1 cm^{-1}) to obtain fine frequency scale for calibration by recoding the FP etalon fringes detected by a photodiode. All the signals are monitored in a 4-channel DSO. The Q-switch output from the Nd:YAG laser is used

for triggering the boxcar averager units and the DSO. The scanning of the dye laser is done using PC with RS 232 interface at a scan step size of 0.001 nm/step.

3 Results and discussion

The ground state of Sm I is represented by the spectral term $4f^6 s^2$ (^7F_J) with seven fine structure multiplets, identified by $J = 0-6$ corresponding to energy levels at 0 cm^{-1}($^7F_0$), 292.58 cm^{-1} ($^7F_1$), 811.92 cm^{-1}($^7F_2$), 1489.55 cm^{-1} ($^7F_3$), 2273.09 cm^{-1} ($^7F_4$), 3125.46 cm^{-1} ($^7F_5$), and 4020.66 cm^{-1} ($^7F_6$). The schematic excitation scheme used in these experiments is given in Fig. 2. Photoionization experiments are performed by tuning the first dye laser (DL$_1$) to the known Sm I atomic transition 0 cm^{-1}($J = 0$) → 15650.5 cm^{-1} ($J = 1$). The excitation of the population from the level at 15650.5 cm^{-1} ($J = 1$) to the second excited level at 33116.8 cm^{-1} ($J = 1$) and further ionization to the continuum are done by using the second dye laser (DL$_2$) via a resonant $\lambda_1 + 2\lambda_2$ process. In these experiments, we have used two different polarizations for the excitation lasers: case (a) when both lasers have parallel linear polarization ($\hat{e}_1 \parallel \hat{e}_2$) and case (b) when λ_1 is circularly polarized while λ_2 is linearly polarized.

The basic principle behind Sm isotope separation technique based on polarization selection rules is schematically shown in Fig. 3a, b. The figures illustrate the possible excitation routes for even and odd isotopes from the ground state of Sm I for parallel linear polarizations of the excitation lasers. The symbols J and M_J denote the total angular momentum quantum number and the magnetic quantum number, respectively. As shown in Fig. 3a, each energy state of an even isotope has $2J + 1$ degenerate magnetic sublevels. The dipole transitions for the linearly polarized (π) radiations are allowed between magnetic sublevels of same M_J except for the symmetry forbidden transition
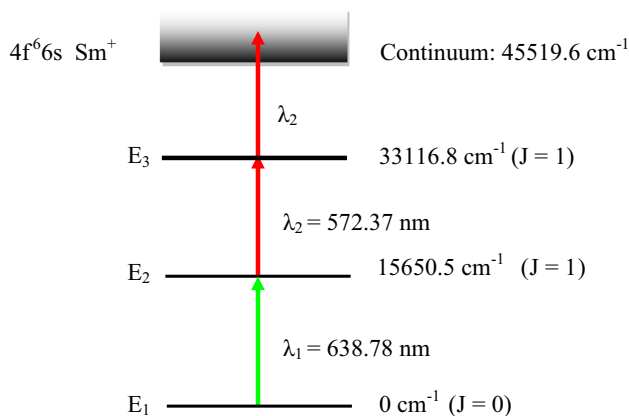
$\Delta J = 0$, $\Delta M_J = 0$, and M_J: $0 \leftrightarrow 0$. Thus, the second-step transition ($J = 1$, $M_J = 0 \rightarrow J = 1$, $M_J = 0$) is forbidden for an even isotope, and hence, the population remains trapped in the first excited state, E$_2$ ($J = 1$), when both the excitation lasers have parallel linear polarization. In the case of an odd isotope, due to nonzero nuclear spin ($I = 7/2$),
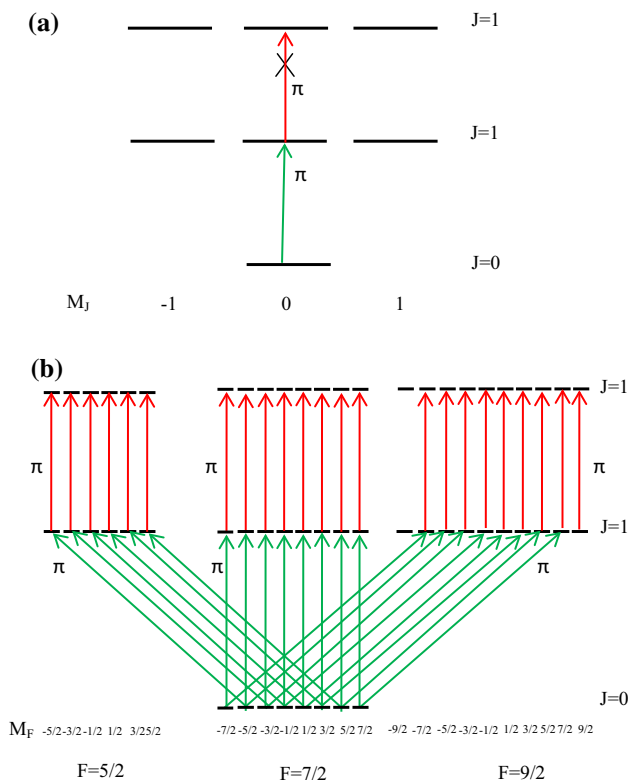

Fig. 3 Transitions between magnetic sublevels of Sm I for parallel linear polarizations of the excitation lasers. **a** Even isotope **b** odd isotope for the chosen scheme. Forbidden transition is labelled with a cross
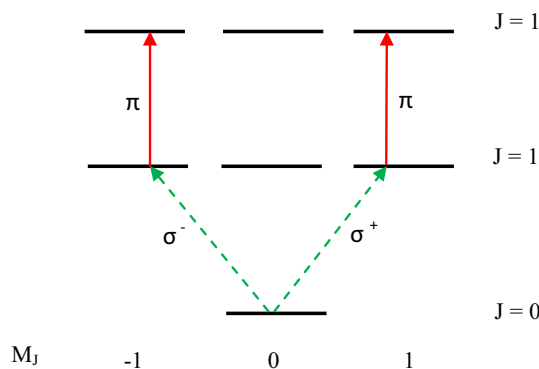

Fig. 2 Excitation scheme

Fig. 4 Transitions between magnetic sublevels of Sm I in case of an even isotope when λ_1 is circularly polarized and λ_2 is linearly polarized

there is hyperfine interaction between J and I and hence F becomes the good quantum number instead of J resulting in hyperfine structure for the energy state. For example, the excited state ($J = 1$) splits into three ($F = 5/2$, $F = 7/2$, and $F = 9/2$) hyperfine energy levels. Each hyperfine state has $2F + 1$ degenerate magnetic sublevels M_F as shown in Fig. 3b. Transitions between the magnetic sublevels satisfying $\Delta M_F = 0$ for $\Delta F = 0, \pm 1$ are then allowed in this case with the exception of the transition $\Delta F = 0$, $\Delta M_F = 0$, and $M_F = 0 \leftrightarrow 0$. Thus, there are possible excitation pathways to the excited level E_3 ($J = 1$) in the case of an odd isotope. Conversely, if any one of the excitation lasers is circularly polarized, due to the M_J selection rule of $\Delta M_J = \pm 1$ for circularly polarized light, the yield of the even isotope will be nonzero. For example, Fig. 4 illustrates the transitions between magnetic sublevels of even isotopes in case when the first-step laser is circularly polarized and the second laser is linearly polarized. Hence, isotope-selective excitation of the odd isotopes is possible when appropriate combinations of J values and laser polarizations are used.

Two-color photoionization spectroscopy of Sm I is performed for two different cases of polarizations of the excitation lasers while keeping all other experimental parameters unchanged. The TOF-mass spectra of the photoions produced when (a) both λ_1 and λ_2 lasers have parallel linear polarization and (b) λ_1 is circularly polarized and λ_2 is linearly polarized are shown in Fig. 5a, b, respectively. In case (a), selective ionization of the two odd isotopes of Sm (^{147}Sm and ^{149}Sm) could be seen very clearly, whereas, in case (b), we have observed non-selective photoionization. The observed isotopic ratio (^{149}Sm/^{152}Sm) measured in case (a) is ~40, and in case (b), it is ~1. It may be noted that the mass spectrum observed in Fig. 5b does not reflect the natural abundance since it depends on where exactly the peak centre of the first-step laser is fixed in between the resonance of ^{144}Sm and ^{154}Sm isotopes and also on the polarization characteristics of the excitation lasers. Thus, using parallel linearly polarized lasers, for the chosen two-color photoionization scheme of Sm I, the isotopic selectivity, which is defined in these studies as the ratio of the observed abundance of ^{149}Sm/^{152}Sm in case (a) to case (b), of ~40 is achieved. It may be added that when compared with the natural abundance ratio of ^{149}Sm/^{152}Sm of 0.52 the selectivity obtained in case (a) will be approximately 77.

To corroborate it further, we have recorded the mass-resolved two-color photoionization spectrum of odd and even isotopes with polarizations of $\hat{e}_1 \parallel \hat{e}_2$, by keeping the boxcar averager gates on the mass peaks corresponding to the odd and even isotopes (^{149}Sm and ^{152}Sm). In this experiment, λ_1 was tuned to the Sm I atomic resonance 0 cm^{-1} ($J = 0$) $\rightarrow$ 15650.5 cm^{-1} ($J = 1$) and λ_2 was scanned from 570 to 573 nm. The mass-resolved two-color
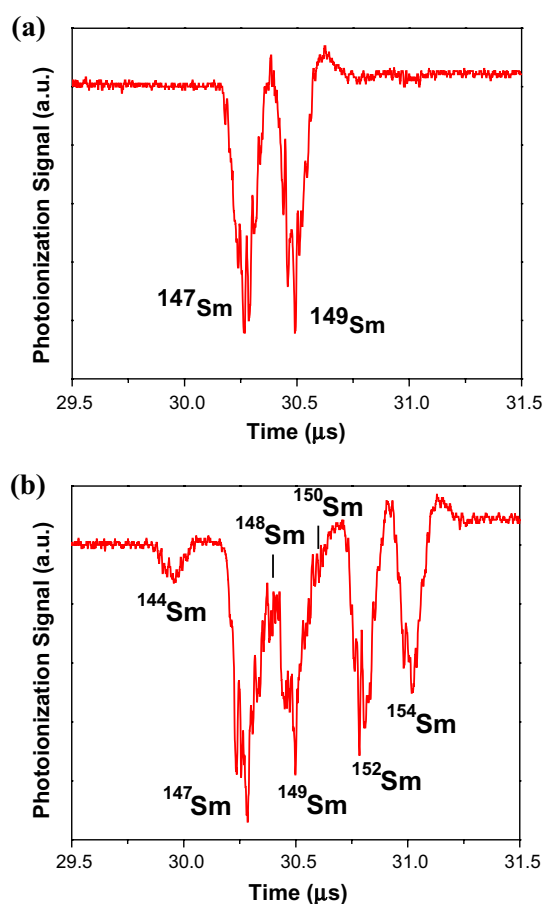

Fig. 5 Two-*color* photoionization mass spectra **a** when both λ_1 and λ_2 lasers have parallel linear polarization and **b** when λ_1 is circularly polarized and λ_2 is linearly polarized
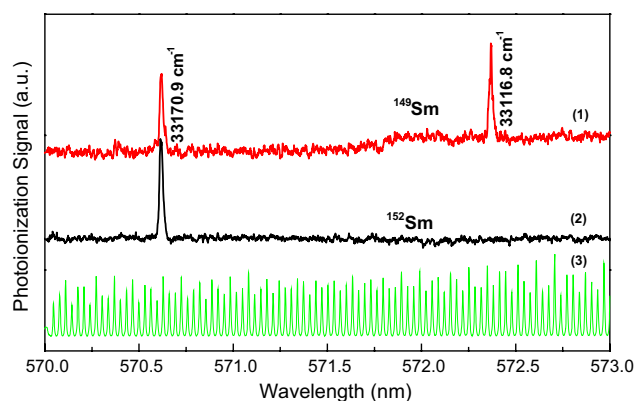

Fig. 6 Mass-resolved two-color photoionization spectra of Sm I. (1) Two-color photoionization spectra for the odd isotope (^{149}Sm), (2) two-color photoionization spectra for the even isotope (^{152}Sm), and (3) Fabry-Perot etalon fringes

photoionization spectrum observed is shown in Fig. 6. The resonance at 572.37 nm corresponds to the high-lying level at 33116.8 cm^{-1} ($J = 1$), previously reported in the

literature [12], and the second resonance at 570.60 nm corresponds to a new level at 33170.9 cm^{-1} with probable J value of 0 or 2. These resonances are verified as two-color resonances by blocking the first-step laser so that the photoionization signal disappears completely. During these experiments, the second-step dye laser fluence was kept low (~300 μJ cm^{-2}) so that it did not produce any single-color multi-photon ionization. It may be seen in Fig. 6 that the resonance at 572.37 nm has appeared only in the spectrum of the odd isotope confirming the selective photoionization. It is observed that the isotopic selectivity degrades with increasing power of the excitation lasers due to multi-photon ionization process.

We have also investigated the effect of relative polarization angle between the two linearly polarized lasers on the ionization yield for even and odd isotopes. In this case, for the chosen excitation scheme, the first laser induces an electronic transition from an initially isotopic ground state |jm> to an excited state |JM>. This population alignment produced by the first laser is probed by a second laser for which, the electric field makes an angle θ with respect to the polarization axis of the first laser. Theoretical considerations show that the square matrix element for the second-step transition $J_2 \rightarrow J_3$ is proportional to

$$
|W_{J_2 J_3}|^2 \propto \left[\left(\frac{\sin\theta}{\sqrt{2}} \right)^2 \begin{pmatrix} 1 & 1 & 1 \\ 1 & 0 & -1 \end{pmatrix}^2 + (\cos\theta)^2 \begin{pmatrix} 1 & 1 & 1 \\ 0 & 0 & 0 \end{pmatrix}^2 \right.
$$
$$
\left. + \left(-\frac{\sin\theta}{\sqrt{2}} \right)^2 \begin{pmatrix} 1 & 1 & 1 \\ -1 & 0 & 1 \end{pmatrix}^2 \right] \propto \sin^2\theta \qquad (1)
$$

Due to this redistribution of atoms between the magnetic sublevels on changing the quantization axis [13–16], the second-step transition, which is forbidden for $\hat{e}_1 \parallel \hat{e}_2$ polarization in case of an even isotope, becomes allowed for different orientations of $\hat{e}_2$ with respect to $\hat{e}_1$, thus degrading the selectivity of the process.

The photoionization yield for odd and even isotopes is measured as a function of relative polarization angle between first- and second-step lasers for the chosen photoionization scheme. The ion yield for the odd isotopes does not show significant dependence on the relative polarization angle. The ratio of even to odd isotope (^{152}Sm to ^{149}Sm) photoionization yields as a function of polarization angle between two lasers is shown in Fig. 7. The dependence of the even mass isotope signal on the relative polarization angle followed $\sin^2\theta$, which is in excellent agreement with theoretical predictions. Degradation in the selectivity of the process as the relative polarization angle between the two lasers is rotated from linear to perpendicular is observed with a minimum selectivity at a relative polarization angle of 90 ° between the two lasers.
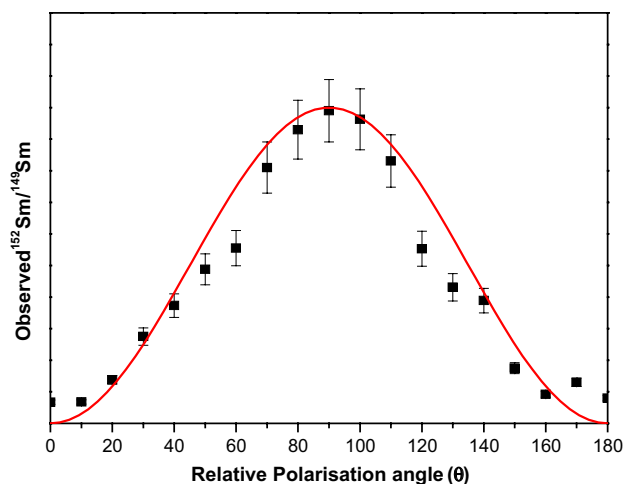

Fig. 7 Dependence of the ratio of the photoionization signal for the even isotope to that of the odd isotope (^{152}Sm/^{149}Sm) on relative polarization angle (θ) between the two dye lasers

4 Conclusions

Polarization-based isotope-selective photoionization of odd isotopes of Sm I has been investigated by using two-color three-photon photoionization spectroscopy with broadband lasers. We have experimentally demonstrated an isotopic selectivity of more than 40 between the odd and even isotopes of atomic Sm by judiciously selecting proper excitation sequence and polarizations of the excitation lasers. To our knowledge, this is the first experimental demonstration of isotope-selective excitation of odd isotopes of samarium using polarized laser beams. Since the technique has the advantage that the isotopic selectivity is not affected by the spectral broadening of the excitation lasers, it is highly useful for the separation of odd and even isotopes exhibiting overlapping spectra owing to small isotope shifts and broad hyperfine structures. We have also studied the effect of different states of polarization of the excitation lasers and the relative polarization angle between them on the isotopic selectivity.

References

1. H. Niki, T. Kuroyanagi, Y. Horiuchi, S. Tokita, J. Nucl. Sci. Technol. **6**, 101 (2008)
2. H. Niki, J. Korean Phys. Soc. **56**, 190 (2010)
3. E. Le Guyadec, J. Ravoire, R. Botter, F. Lambert, A. Petit, Opt. Commun. **76**, 34 (1990)
4. C.A. Haynam, B.J. Comaskey, J. Conway, J. Eggert, J. Glaser, E.W. Ng, J.A. Paisner, R.W. Solarz, E.F. Worden, Proc. SPIE **1859**, 24 (1993)

5. H. Niki, K. Motoki, M. Yasui, Y. Horiuchi, S. Tokita, Y. Izawa, J. Nucl. Sci. Technol. **43**, 427 (2006)

6. H. Niki, T. Kuroyanagi, K. Motozu, Jpn. J. Appl. Phys. **48**, 116510 (2009)

7. G.I. Bekov, A.N. Zherikhin, V.S. Letokhov, V.I. Mishin, V.N. Fedosov, JETP Lett. **33**, 450 (1981)

8. L.C. Balling, J.J. Wright, Appl. Phys. Lett. **29**, 410 (1976)

9. J.A. Ransohoff, U.S. Patent, 3,103,479 1963

10. J.-P.A. Renier and M.L. Grossbeck: Development of improved nuclear poisons for commercial nuclear power reactors, ORNL/TM-2001/238 63 (2001)

11. W.C. Martin, R. Zalubas, L. Hagan: Atomic energy levels-the rare-earth elements (Natl. Stand. Ref. Data. Ser., circ. 60 Natl. Bur. Stand., Washington, DC, 1978)

12. T. Jayasekharan, M.A.N. Razvi, G.L. Bhale, J. Opt. Soc. Am. B **13**, 641 (1996)

13. M.P. Chernomorets, M.V. Dubov, G.V. Klishevich, Opt. Commun. **171**, 253 (1999)

14. R.N. Zare, *Angular momentum* (Wiley, New York, 1988)

15. L.W. Green, G.A. McRae, J.H. Rowat, Inst. Phys. Conf. Ser. **114**, 113 (1990)

16. L.W. Green, G.A. Mcrae, P.A. Rochefort, Phys. Rev. A **47**, 4946 (1993)